Automated Detection of Hazardous Sea Ice Features from Upward Looking Sonar Data

David Fissel, Anudeep Kanwar, Keath Borg, Todd Mudge, John Marko and Adam Bard
ASL Environmental Sciences Inc.
Sidney, B.C. Canada V8L 5Y3
dfissel@aslenv.com

ABSTRACT

Upward-looking sonar (ULS) instruments provide extended continuous measurements of ice thicknesses and ice velocities, over thousands of kilometers of ice provide important data for establishing metocean design criteria related to oil and gas operations in areas with seasonal or year-round ice cover. This paper describes the development of algorithms for the detection and measurement of hazardous ice features including: large individual ice keels with thicknesses of 5 to well over 20 m; long sections of thick hummocky (rubble) sea ice; and occurrences of multi-year ice floes. Large individual ice keels are detected using an ice draft threshold technique to identify very thick ice floes which are then categorized as to total width using a Rayleigh criteria and/or a minimum user-specified threshold value (e.g. 2 m). The detection of thick hummocky ice is based on minimum criteria of ice draft data segments having median values exceeding 2.5 m and segment lengths exceeding 100 m. For qualifying segments, a selection parameter γ, defined as the 90th percentile over the 50th percentile value of ice drafts divided by the standard deviation was computed; hummocky ice is characterized by $\gamma > 2$ and is also very common for $1.5 < \gamma < 2$. Results from the ongoing algorithm development for detection of multi-year ice features will also be discussed. Ice velocities can also pose difficulties for offshore oil and gas operations in terms of floating drilling platform station keeping when particularly large ice speeds occur and/or ice drift directions changing rapidly or erratically.

KEY WORDS: sea-ice, keels, draft, thickness, multi-year ice, hummocky, sonar;

INTRODUCTION

Starting in 1996 for oil and gas applications in Sakhalin Territory, Russia, upward-looking sonar (ULS) instruments have become the primary source of data for extended measurements of sea ice thickness, to accuracies of 0.05 m, as well as for detailed characterization of keel shapes and other ice features (Fissel et al., 2008b). ULS instruments, in the form of ASL's Ice Profiler, have the data capacity and accuracy/resolution sufficient for unattended operation for periods of up to three years. When combined with a companion Acoustic Doppler Current Profiler (ADCP) to measure ice velocities, the instruments provide horizontal resolution as good as 0.5 m.

The combined ice thicknesses and ice velocities, measured along thousands of kilometers of ice which typically move over each moored ice profiler location, provide important data for establishing metocean design criteria related to oil and gas operations in areas with seasonal or year-round ice cover. Hundreds of ice ULS deployments have been made with these instruments in the ice infested areas of the northern and southern hemispheres (Fissel et al., 2008a).

In recent years, real-time measurements of ULS instrument arrays have been developed and operated in support of shipping and offshore oil and gas exploration. For these applications, there is a need for automated detection of hazardous sea ice features which are embedded within the thousands of kilometers of sea ice passing the measurement site. In this paper, we present the basis for the development of algorithms used in the detection and measurement of hazardous ice features. The types of hazardous ice features that can be detected are:

(a) large individual ice keels with thicknesses of 5 to well over 20 m;
(b) long sections of thick hummocky sea ice; and
(c) occurrences of multi-year ice floes
(d) large ice speeds combined with rapidly changing ice velocity directions.

The methods developed to detect hazardous ice features, and examples of the results, are presented. Recommendations are provided for the development of further enhancements to these algorithms.

UPWARD LOOKING SONAR MEASUREMENTS

Instruments

The upward looking sonar instrumentation, consisting of the Ice Profiler Sonar (IPS) and the Acoustic Doppler Current Profiler (ADCP) are designed to be deployed 25 to 50 m below the air water interface from sea floor based moorings (Figure 1) or, in shallower water, from bottom-mounted platforms. As developed in the early 1990's (Melling et al., 1995) the instrument operated by emitting and detecting surface returns from frequent short pulses (pings) of acoustic energy concentrated in narrow beams (less than 2° at half power). Precise measurements of the delay times between ping emission and reception were converted into ranges separating the instrument's transducer and the ice undersurface. Contemporary data from the instrument's on-board pressure sensor were then combined with atmospheric surface pressure data and estimates of the mean sound speed in the upper water column (obtained from data collected during absences of ice above the instrument) to derive estimates of ice draft from each emitted ping.

Ice Draft Data

When deployed under moving ice fields with adjacent upward-looking

ADCP (Acoustic Doppler Current Profiler) instruments (Figure 1) with capabilities for extracting of ice drift velocity, the obtained data are used to construct two dimensional cross-sections of the ice cover (Figure 2), designated as quasi-spatial profiles. With careful processing these products depict detailed variations in the depth of the lower ice surface with a horizontal resolution of about 1 m and an accuracy in the vertical of 5-10 cm. Keys to the utility of the technique are its on-board data storage capacity and capabilities for reliable long term un-attended operation in the hostile environments usually associated with ice covered waters. Until recently, principal users of this technology have been polar ocean scientists with interests and concerns regarding climate change (Fissel et al., 2008a) and, increasingly, international oil and gas producers with deployments throughout the Arctic Ocean and in sub-polar seas (Figure 3)
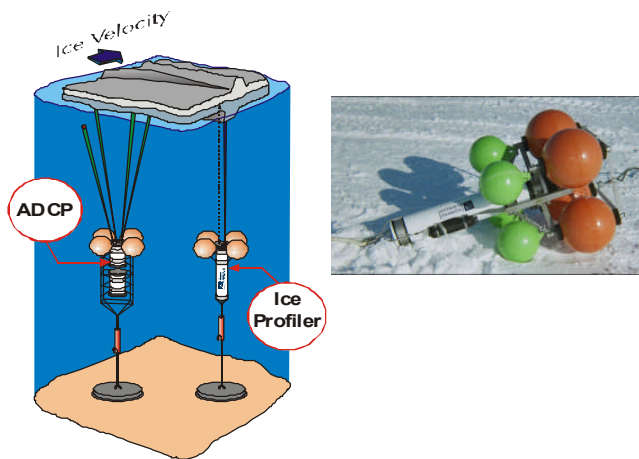

Figure 1. A typical deployment arrangement of an ice profiler and ADCP ice velocity measuring instruments on separate, sea floor-based, moorings.
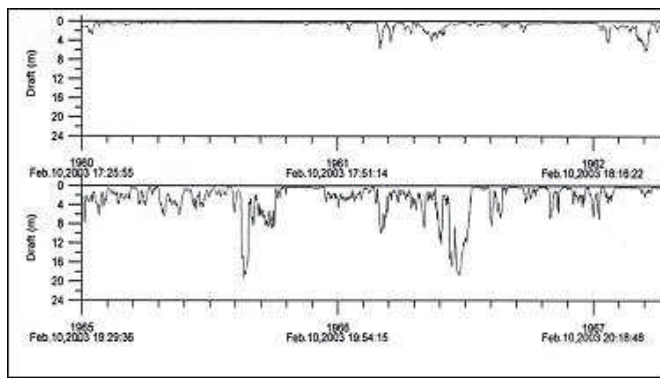

Figure 2. A quasi-spatial profile of an ice cover produced by combining time series draft and ice speed data to produce a product equivalent to the profile of the ice undersurface along a line traced out by all points on the ice which move over the ice profiler instrument during the measurement period. The abscissa is in kilometers, annotated with time of observation.

A new generation of Ice Profiler instruments became available in 2007 (Fissel et al., 2007) which provide enhanced capabilities for sea-ice measurements in the form of more data storage capacity, better resolution and the capability to measure the acoustic backscatter returns beneath and into the ice in addition to the target range to the underside of the sea-ice.
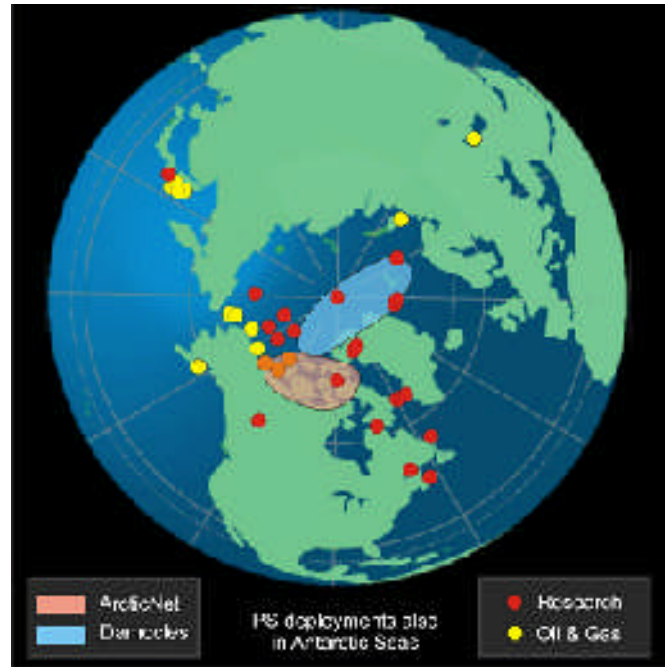

Figure 3. Locations of marine moored ice profiler deployments in the Northern Hemisphere from 1996 to the present. Ice profiler locations for scientific applications are shown by red and orange symbols while oil and gas locations are shown by yellow symbols. The orange symbols designate the locations of long term ice profiler measurements in the Beaufort Sea of the Dept. of Fisheries and Oceans (Dr. H. Melling) which have been used by oil and gas companies.

LARGE INDIVIDUAL ICE KEELS

Each large ice keel in the ice data sets is identified from special scanning software applied to the 1.0 meter resolution ice draft spatial series. Typically three sets of large ice keels are identified according to user-selected threshold values for the maximum ice draft value that each ice keel must exceed. Typically, the ice keels of interest are those with ice drafts that exceeded 5, 8 and 11 m in draft.

Methodology for Identifying Ice Keels

Starting with the 1 m resolution spatial series, a 5 point moving average filter was applied to the spatial series to reduce the high frequency variability. This smoothed spatial series was examined to locate ice keels. The keel detection algorithm was based on Criterion A as described in Vaudrey (1987). Ice keels that exceeded 5, 8 and 11 m were identified using either a Rayleigh criterion (α = 0.5) or a lower threshold of 2 m to end a feature. Figure 4 shows an example of a keel detected using this algorithm.
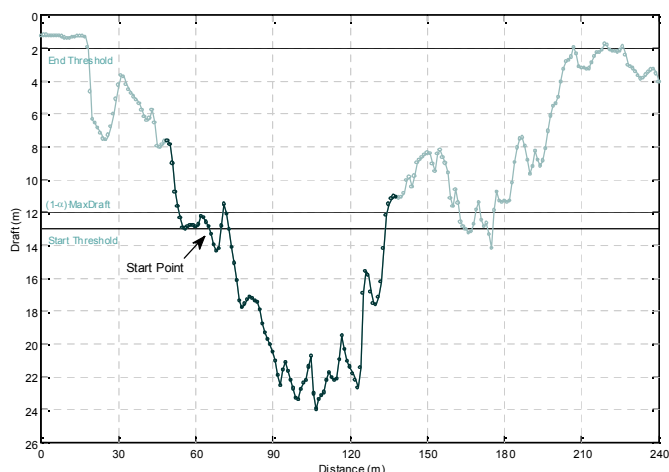.

Figure **4**: An example of the thresholds used by the keel identification algorithm. The keel was found using a start threshold of 13 m and an end threshold of 1 m and α set to 0.5

For illustrative purposes, a 13 m starting threshold is used in the figure. A keel started, shown as **Start Point** in the figure, once the draft exceeded the **Start Threshold**. The data was read from this crossing point to determine the maximum draft until a point was found to end the feature. The keel ended if it crossed the **End Threshold** or if it reversed slope past a threshold given by **(1 - α)*Maximum Draft**. Once the end of the keel was found, the data points were scanned backwards in the file from the **Start Point** until the beginning of the keel was found. The keel start point was found if it crossed the **End Threshold** or if it reversed slope past the threshold given by **(1 - α)*Maximum Draft**. Unlike the forward search to find the keel endpoint, the maximum draft was not updated; instead the value found for the forward search was used.

The backwards search technique used to find the start of a keel can result in overlapping keel features when a keel with a larger maximum draft was followed by one with a lower maximum draft. In the backwards search on the second lower draft keel, the beginning of the keel can extend past the beginning of the first keel since the lower draft means a lower α threshold. It is also possible that the second keel can overlap with more than one previous feature. After the preliminary keels were selected, they were re-processed and the overlapping features were combined into a single event by using the start of the first keel in the overlap and the end of the last keel in the overlap. An example of this type of overlap and the resulting combined feature is shown in Figure 5. For illustrative purposes, a 13 m starting threshold was used. Figure 5 shows an overlap with the feature in Figure 4 and the effect of combining the two features.

Description of the Database of Ice Keel Features

A database of keel features was derived using 5, 8, and 11 m starting thresholds, a 2 m end threshold, and a α = 0.5 Rayleigh criterion. Data files were created for each spatial segment and start threshold and contained one entry for each detected keel. A description of the fields in this file is provided in Table 1.
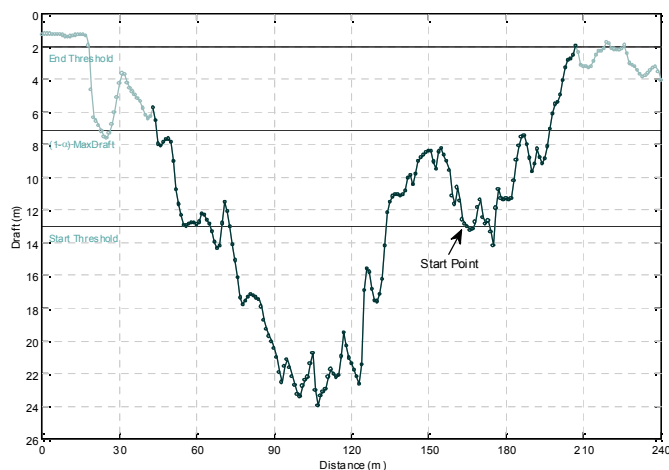

Figure 5: example of a keel feature extending from the Start Point beyond the feature shown in Figure 4.

Data files were created that contained statistical results calculated for monthly and ice season time periods for each start threshold. A description of the fields is provided in Table 2.

Table 1: A description of each field in the keel feature data file.

Field	Description
Start Time	The start time of the segment (seconds). The actual date of this segment can be obtained by adding the start date in the Header file to this record.
End Time	The end time of the segment (seconds). The actual date of this segment can be obtained by adding the start date in the Header file to this record.
Start Distance	The start distance value from the input ice draft data file (m).
End Distance	The end distance value from the input ice draft data file (m).
Width	The width of the keel feature (m).
Mean Draft	The mean draft value of the keel feature (m).
Maximum Draft	The maximum draft value of the keel feature (m).
Minimum Draft	The minimum draft value of the keel feature (m).
Std Dev of Draft	The standard deviation of the draft of the keel feature (m).

Table 2: A description of each field in the keel statistics (by segment) data file.

Field	Description
Start Time	The start time of the statistic segment (seconds). The actual date of this segment can be obtained by adding the start date in the Header file to this record.
End Time	The end time of the statistic segment (seconds). The actual date of this segment can be obtained by adding the start date in the Header file to this record.
Min of Max Draft	The minimum of all the maximum keel segment drafts in the time period (m).
Mean of Max Draft	The mean of all the maximum keel segment drafts in the time period (m).
Max of Max Draft	The maximum of all the maximum keel segment drafts in the time period (m).
Std of Max Draft	The standard deviation of all the maximum keel segment drafts in the time period (m).
Mean of Mean Draft	The mean of the entire mean keel segments drafts in the time period (m).
Std of Mean Draft	The standard deviation of the entire mean keel segments drafts in the time period (m).
Min Width	The minimum of all the keel segment widths in the time period (m).
Mean Width	The mean of all the keel segment widths in the time period (m).
Max Width	The maximum of all the keel segment widths in the time period (m).
Std of Width	The standard deviation of all the keel segment widths in the time period (m).
Total Ice Distance	The total distance of ice covered for the time period (m). This total distance includes all non-flagged data (ice).
Tot Ice + O/W Dist	The total distance of ice and open water covered for the time period (m). This total distance includes ice and data flagged as open water (-100).
Total Distance	The total distance covered for the time period (m). The total distance includes ice, data flagged as open water (-100) and data flagged as bad (-200, -500 and -9999).
Sum of Keel Widths	The sum of the keel widths for the time period (m).
Sum of Keel Areas	The sum of the keel areas for the time period (m²). The area is calculated from the sum of the product of the mean draft and the width of each segment.
Number of Keels	The number of keel features in the time period.

Large Ice Keel Results

An example of the results for large ice keels, as analyzed at the long term measurement location site 2 located on the outer edge of Canadian Beaufort Sea shelf (Melling et al., 2005) in a water depth of 90 to 100 m.

A subset of the monthly summary statistical parameters for large ice keels are presented in Table 3 for the 2006-2007 ice season at site 2 for the 5 m ice draft threshold. In this 12 month period, 5,554 individual large ice keels were identified and extracted from the spatial ice draft data series. These large ice keels spanned a total distance of 2,931 km. The number of large keels for the 8 m and 11 m threshold ice draft value were 1,346 and 335. The maximum measured ice draft was 26.57 m, in May, with ice keel drafts exceeding 20 m occurring in the summer (July). The average width of the large ice keel features were 31.1 m (5 m threshold), 34.7 m (8 m) and 46.2 m (11 m). The maximum monthly width of these large ice keels is typically 100 – 150 m, although a few keels are identified as having widths of over 300 m. The ice keels having widths of more than 100-200 m likely include hummocky or old ice features which are discussed later in this paper.

Table 3: Site 2 2006-2007 Monthly Statistics for the 5 m ice draft threshold value.

Mon.	Maximum Draft		Width		Distance		Keels
	Mean	Max	Mean	Max	Total Ice	Total O/W	Number
	(m)	(m)	(m)	(m)	(km)	(km)	
5 m							
Oct.	5.65	5.66	13	16	492	18	2
Nov.	6.53	14.78	27.57	119	384	0	312
Dec.	6.88	18.18	32.09	387	480	0	977
Jan.	6.79	18.31	29.72	118	214	0	693
Feb.	6.65	15.98	28.82	146	221	0	404
Mar.	6.99	17.89	32.08	101	60	0	250
Apr.	7.11	22.69	30.66	161	285	0	873
May	7.9	26.57	38.27	265	286	0	915
June	7.14	21.37	36.22	355	372	192	650
July	7.89	22.83	53.53	349	114	158	438
Aug.	6.23	9.45	33.6	106	21	321	35
Sept.	6.5	8.61	17.6	34	3	76	5

The occurrence of large ice keels is highly episodic on daily time scales as shown in Figure 6. The duration of events where more than 10-20 ice keels occur on consecutive days range from a few to several days.
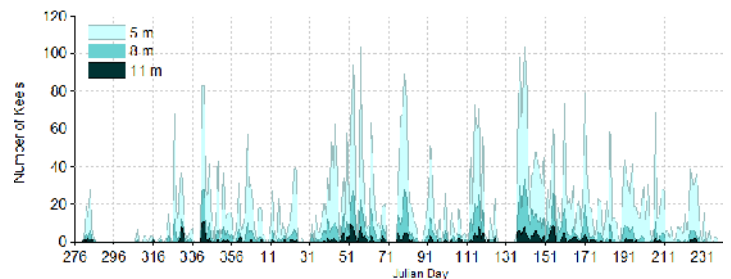
Figure 6: Daily Keel Number for Site 2 2006-2007.

HUMMOCKY (RUBBLED) SEA ICE

Hummocky (sometimes referred as ice rubble fields) sea ice represents a different type of deformation of first year sea ice from the heavily ridged large ice keel features described above. Distinctions between hummocky and ridge sea ice are not easy to establish and are based on the underlying deformation mechanism for each ice type: with hummocky ice originating primarily from compressive events which force adjacent floes to ride up or slide over each other while ridged ice tends to arise from more drastic events in which floes are crushed and turned so that their original planes are oriented well off the vertical direction to produce more linear and more localized deformations which are usually more extensive in the vertical dimension (Fissel et al., 2008).

Automated methods for detecting hummocky ice were derived from analysis of several ice profiler sonar (IPS) data sets from the Canadian Beaufort Sea in May through November over 2002 and 2006. The spatial series of ice drafts, having 1 m spacing as derived from the IPS and ADCP measurements, were used. An algorithm was developed which could distinguish between "hummocky" and "ridged" (or large keels) portions of the ice cover. Distinctions between these two categories are not easy to establish but largely derive from the underlying deformation mechanism as described above. The end result is that hummocky sections do not have large, drastic variations in draft and tend to be smoother while undulating about a particular value, or constrained to relatively similar draft values. The spatial ice draft series were examined for continuous segments of hummocky ice, initially identified by satisfying 3 criteria:
1) The minimum draft is no lower than 1m
2) The segment maintains this minimum draft for at least 100m in distance
3) The 50th percentile draft is at least 2.5 m.
Although these 3 criteria alone identified many hummocky segments, it failed to uniquely identify them. Many segments were also characterized by high degrees of ridging through the appearance of distinct large keel features. An additional criteria was added that
4) The segments are free of any keels already identified in the large keel database.

The segments that satisfied all these criteria were deemed to be consistent with the description of hummocky ice in the majority of cases. In the process of trying to identify these segments, various measures of the spread of the draft distribution were examined to determine if there were any statistical features which were common to hummocky segments. Although the most evident choice would be the standard deviation, the segments generally had non-Gaussian distributions; this was therefore impractical in application.

Dividing out two measures of the spread, i.e. the 90th percentile over the 50th percentile value all over the standard deviation, gave a parameter, γ, which was found to be fairly reliable at distinguishing between hummocky segments. This parameter gives a reasonably good estimate of the probability that a segment fits the description of hummocky ice. Segments with large keels tend to have a large 90th percentile to 50th percentile value, but the standard deviation would also tend to be quite high, so it could be expected that γ would be low in these cases. For hummocky ice segments, the 90th to 50th percentile value would tend to be lower but the standard deviation would be low resulting in a higher value of γ. The main advantage of using γ is that it allows for an easier global comparison between segments and seems to eliminate the variability that arises when comparing non-Gaussian distributions of drafts. Typically, the following thresholds were found for γ:

$\gamma > 2$: The probability that the segment fits the description of hummocky ice is very high. In these cases the standard deviation is comparatively low, so the ice segment would tend to be fairly level.
$\gamma < 1$: There are large keels present in the segment and the probability that it is hummocky ice is q low. The sizes of the keels are quite large compared to the 50th percentile value, but the standard deviation is also high, resulting in a low gamma.

These two cases work reasonably well as a first approximation. For intermediate values, a histogram of the draft records in the segment needs to be examined before determining whether the segment is hummocky ice. These segments could be broken down as:

$1.5 < \gamma < 2$: Usually hummocky ice, but could also be a small keel (less than keel database threshold) surrounded by level ice of a relatively similar value
$1.0 < \gamma < 1.5$: Not usually hummocky ice, keels are much larger than median or surrounding values. May have a tail, or broader distribution.

It appears that γ can classify the probability of hummocky ice for values increasingly well for values greater than 2. Hummocky ice segments may also occur for the intermediate values of gamma, but require visual examination of the plots and parameters as an additional check.

Table 4 is a joint frequency distribution of γ vs. the number of keels found in each of the segments which satisfy the initial 3 criteria described above. This table shows that higher values of γ are almost exclusively found in segments with fewer keels. For example, there are 115 segments that have $1.8 < \gamma < 2.0$; 82 of them have no keels, 25 have 1 keel and 8 with 2 keels. As γ values increase to the right, most segments have no keels while a few have 1 keel. For values of $\gamma > 2.4$, only segments free of keels are found. Moving to lower γ values, it is clear that segments with more keels have a lower γ. It is therefore recommended that γ could be used in future studies as a first estimate to find hummocky ice segments.

Table 4: Joint Frequency Distribution of occurrences for γ vs. the number of ridged keels.

Min γ	0.2	0.6	1.0	1.4	1.8	2.2	2.6	>3	
Max γ	0.6	1.0	1.4	1.8	2.2	2.6	3.0		
No.Keels									Total
0	0	0	17	118	172	100	42	35	484
1	19	73	191	198	31	2	0	0	514
2	12	87	141	71	8	0	0	0	319
3	6	60	62	23	0	0	0	0	151
4	4	39	56	13	0	0	0	0	112
>5	3	32	21	1	0	0	0	0	57
Total	44	291	488	424	211	102	42	35	1637

In Figure 7, some examples of hummocky ice segments are presented from the Beaufort Sea in 2006. These segments fit the description of hummocky ice outlined earlier quite well. They do not exhibit large, drastic variations in draft and are generally constrained to relatively similar draft values. Histograms of the number of draft values are presented alongside each segment as well as the segment's γ value, which are generally around 2. Both of these can be used as a further test to assess the validity of the segment's classification as hummocky ice. It is worth noting that there were a few segments that satisfied all the above criteria but were extremely flat, level sections of ice with essentially little or no variation in draft value. These segments appear to be the underside of smooth, large keels but have a much larger coherence length (distance between peak draft values) than a more typical hummocky ice segment.

MULTI-YEAR ICE FLOES

While first year ice is the dominant ice type in the Arctic Ocean, some of the sea ice is older having survived at least one summer. Old ice has two categories: second year ice and multi-year ice. The latter ice type has survived over two summers. In practice due to the difficulty of distinguishing between second year and old ice, multi-year ice is often associated with any ice that has survived one summer in the Arctic Ocean. As sea ice ages from year to year, its physical properties change (Wadhams, 2000). The salinity is reduced as the brine channels are evacuated and frozen over. The hardness of the ice increases and it yields less to external objects such as ships making passage through the ice, leading to the hazardous nature of this type of ice. The topography of the ice also changes as it becomes smoother on its top and bottom sides.

Detection of old (second- or multi-year ice) from upward looking sonar data sets is challenging. There are two basic approaches that can be used

(a) determination of the roughness scales of the underside of the sea-ice to differentiate between the smoother old ice from the rougher first year ice which involves analysis of ice drafts from several successive pings to determine a bottom roughness scale;

(b) analysis of the details of the acoustic backscatter return realized from each individual acoustic ping.
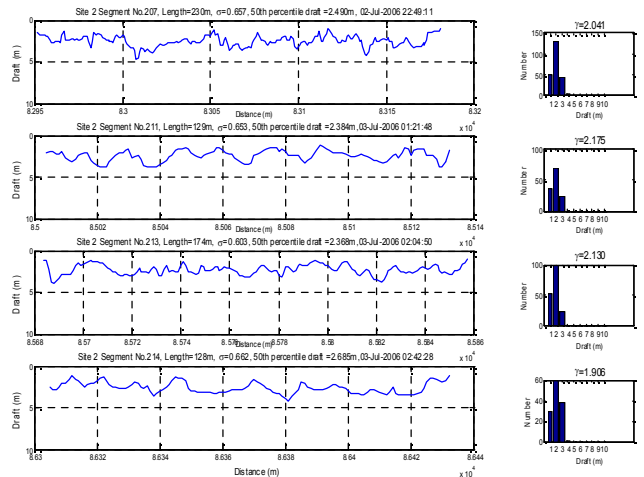

Figure 7, Examples of Hummocky Ice Segments from the Beaufort Sea in 2006. Left figures: Spatial series segment found in IPS record, Right figures: Histogram of draft values in corresponding segment.

The underlying difference in the acoustic return between first year and old ice of the second approach (b) can be seen in Figure 8. For first year ice, the acoustic backscatter returns tend be lower in amplitude relative to that of open water returns and also has a greater penetration of the energy into the underside of the sea ice. In contrast, the harder old ice tends to result in a larger amplitude return as well as a shorter rise time on to the peak amplitude. It should be noted that the use of the detailed backscatter return characteristics is available only for the latest (model 5) of the Ice Profiling Sonar instrument. As this detailed amplitude return envelope information requires considerably more data storage than regular target range only pings, the special pings are typically acquired less frequently (typically once every 15-30 seconds) than regular pings.

Analysis is ongoing to define the respective capabilities of each of the two approaches for detection of old ice. A combination of the two approaches will likely emerge as the optimal method to detect old ice.
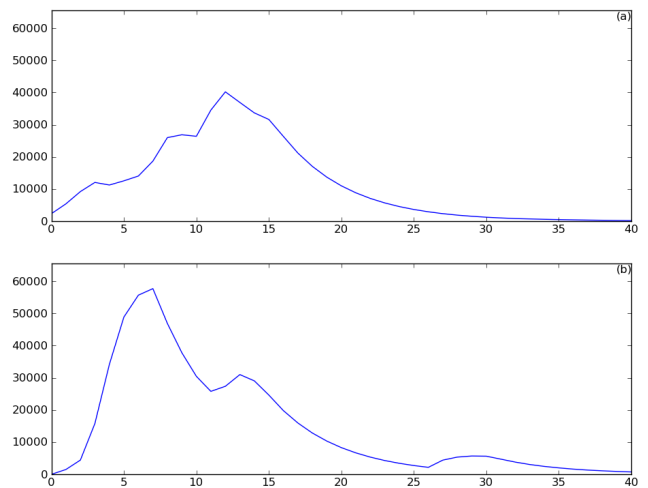

Figure 8: The acoustic backscatter return from individual pings for two different sea ice targets: (a) from first year ice and (b) from old ice.

ICE VELOCITIES

For a moored drilling ship, ice velocities can pose hazards to operations. High ice speeds are clearly one challenge. In the Beaufort Sea, ice speeds can reach values of 0.5 to 1.0 m/s depending on the location. Movements of the sea ice in the form of inertial oscillations represent circular movements of ice floes every 12 hours. Inertial oscillations result in rapidly changing ice velocity directions.

Ice movements involving rapid direction changes, i.e. turning, will put more demands on station keeping and on the ice management operations to support drilling. The nature of ice direction changes during a turning event was examined in terms of the ice draft, ice speed, or event duration. Starting with ice velocity and ice draft data in the Canadian Beaufort Sea in about 50 and 100 m of water by DFO in 2003-2004, and 2005-2007, turning events were examined.

Directional differences spanning one hour were calculated every half hour. An event was defined to be any grouping of consecutive points with direction changes exceeding 20 degrees which, after rejecting the drafts < 0.1m, had a 95 percentile draft exceeding 0.3m, and which had over 100m of ice draft exceeding 0.1m.

The majority of segments found had a maximum hourly change between 20 and 40 degrees. The distribution of absolute direction change versus ice draft (speed) reflected proportionally less ice of deeper draft (ice of faster speed) at each rate change category, as illustrated in Table 1 for the case of mean ice draft. There is no apparent dependence of the direction change on mean ice draft.

As might be expected, one recurring pattern was that the larger the direction difference between the start and end of an event, the longer the duration tended to be. An example of this pattern is shown for the shallow water site 1 for June – December, 2006 in Table 2. Turning events of 30 degrees have a typical duration of about 1-2 hours, while events of 50 to 110 degrees have a typical duration of 2-3 hours, events of 130 to 150 degrees have a typical duration of 4-5 hours and events of 170 to 250 degrees have a typical duration of 5-7 hours. The results suggest that a typical rate of change of ice direction would be about 30 to 45 degrees per hour with a considerable amount of variability exhibited in the analysis results. The estimated rate of change of ice velocity direction with time is roughly consistent with that expected from inertial oscillations (twice daily or 360 degrees divided by 12 hours or ~ 30 degrees per hour).

Table 5: Joint bivariate distribution of the number of turning events for the mean ice draft versus the directional change, for site 1 in the Canadian Beaufort Sea.

Ice Draft (m)	Direction Change during ice turning event							Min. Max. Total
	20 60	60 100	100 140	140 180	180 220	220 260	>260	
0.0	31	8	4	3	1	1		48
0.5	25	2	5	3	1	1	1	38
1.0	27	3		1	1			32
1.5	15	1	2	1				19
2.0	7	2			1			10
2.5	8	1	1	1				11
3.0	7	2						9
3.5	2							2
4.0	6			1				7
4.5	2	1						3
5.0	2			1				3
5.5	1							1
6.0	1							1
6.5								0
7.0	1							1
7.5								0
>7.5	2							2
Total	137	20	12	11	4	2	1	187

Table 6: Joint bivariate distribution of the number of turning events for the duration of the turning event versus the directional change, for site 1 in the Canadian Beaufort Sea.

Event Duration (h)	Direction Change during ice turning event							Min. Max. Total
	20 60	60 100	100 140	140 180	180 220	220 260	>260	
1.0	118	1	2	1				122
2.0	19	15	4	1	1			40
3.0		4	2	3	1			10
4.0			4	3		1		8
5.0				2	3			5
>6						1	1	2
Total	137	20	12	10	5	2	1	187

ACKNOWLEDGEMENTS

REFERENCES

Fissel, D.B., Marko, J.R., Ross, E., Chave, R.A. and Egan, J., 2007. Improvements in upward looking sonar-based sea ice measurements: a case study for 2007 ice features in Northumberland Strait, Canada, in *Proceedings of Oceans '07*, Vancouver, B.C., Canada, 6p. *IEEE Press.*

Fissel, D.B., J.R. Marko and H. Melling, 2008a. Advances in upward looking sonar technology for studying the processes of change in Arctic Ocean ice climate. *Journal of Operational Oceanography*: 1(1), 9-18.

Fissel, D.B, J.R. Marko and H. Melling, 2008b. Advances in Marine Ice Profiling for Oil and Gas Applications. In *Proceedings: IceTech 2008 Conference,* July 20-23, 2006, Banff, Alberta, Canada.

Melling, H., Johnston, P.H. and Reidel, D.L., 1995. Measurements of the Underside Topography of Sea Ice by Moored Subsea Sonar, *J. Atmospheric and Ocean Technology,* 12: 589-602.

Vaudrey, K., 1987. 1985-86 Ice Motion measurements in Camden Bay, *AOGA Project 328, Vaudrey & Associates, Inc.* San Luis Obispo, CA.

Wadhams, P., 2000. Ice in the Ocean. *Gordon and Breach Science Publishers*, Amsterdam, The Netherlands. 351 p.